Computers & Geosciences ▮ (▮▮▮▮) ▮▮▮–▮▮▮

Contents lists available at ScienceDirect

Computers & Geosciences

journal homepage: www.elsevier.com/locate/cageo

Automatic computation of pebble roundness using digital imagery and discrete geometry

Tristan Roussillon [a,*], Hervé Piégay [b], Isabelle Sivignon [c], Laure Tougne [a], Franck Lavigne [d]

[a] Université de Lyon, Université Lyon 2, LIRIS, UMR5205, F-69676, France
[b] Université de Lyon, CNRS, UMR5600, F-69364, France
[c] Université de Lyon, CNRS, Université Lyon 1, LIRIS, UMR5205, F-69622, France
[d] Université de Paris, Laboratoire de Géographie Physique, UMR8591, F-92195, France

ARTICLE INFO

Article history:
Received 19 May 2008
Received in revised form
4 January 2009
Accepted 7 January 2009

Keywords:
Sedimentary particle
Shape description
Discrete geometry
Roundness
Physical abrasion
Bedload transport
River continuum

ABSTRACT

The shape of sedimentary particles is an important property, from which geographical hypotheses related to abrasion, distance of transport, river behavior, etc. can be formulated. In this paper, we use digital image analysis, especially discrete geometry, to automatically compute some shape parameters such as roundness, i.e. a measure of how much the corners and edges of a particle have been worn away.

In contrast to previous work in which traditional digital images analysis techniques, such as Fourier transform, are used, we opted for a discrete geometry approach that allowed us to implement Wadell's original index, which is known to be more accurate, but more time consuming to implement in the field.

Our implementation of Wadell's original index is highly correlated (92%) with the roundness classes of Krumbein's chart, used as a ground-truth. In addition, we show that other geometrical parameters, which are easier to compute, can be used to provide good approximations of roundness.

We also used our shape parameters to study a set of pebbles digital images taken from the Progo basin river network (Indonesia). The results we obtained are in agreement with previous work and open new possibilities for geomorphologists thanks to automatic computation.

1. Introduction

The shape of sedimentary particles is an important property from which geographical hypotheses related to abrasion, distance of transport, river behavior, etc. can be formulated (e.g. Krumbein, 1941). The main shape features are form or sphericity (a sphere similarity measure), roundness (a measure of how much the corners and edges of a pebble have been worn away) and surface texture (a measure of small-scale features) (Barrett, 1980; Diepenbroek et al., 1992).

Roundness of a particle was initially defined by Wadell (1932). This method of estimating roundness is infrequently used even though it is known to be more accurate than other methods (Pissart et al., 1998), because the required number of measurements is time consuming. For each particle, the radius of curvature of each corner has to be measured either on three orthogonal planes or on the silhouette as suggested in the pioneering paper of Wadell (1932). A corner is defined as a part of the contour for which the radius of curvature is lower than the radius of the largest inscribed circle. The ratio between the mean radius of curvature of the corners and the radius of the largest inscribed circle defines the roundness measure (Wadell, 1932) (Fig. 1). No definition of curvature was given in the original paper. In order to shorten the time required to estimate roundness, Krumbein (1941) created a chart (Fig. 2). Krumbein's chart shows examples of pebbles for which the roundness of their silhouette has been calculated using Wadell's method and clusters them into nine classes. Some field guidelines (Bunte and Abt, 2001) recommend a visual estimate of pebble roundness based on the chart. In order to shorten the measurement time while keeping a certain objectivity, some authors have proposed indices that were inspired by Wadell's index, but easier to calculate (e.g. Cailleux, 1947). Pissart et al. (1998) found that the Cailleux and Krumbein methods give similar results on average, with the Krumbein method being much quicker.

Our objective is to reduce the subjectivity and time required for the estimation of pebble roundness by providing an automatic computation method for Wadells index. It is usually computed in the maximum projection plane, "perhaps largely because of the impracticality of measuring true 3D roundness", according to Barrett (1980, p. 300). Even if roundness may be now computed in 3D with laser scanner (Hayakawa and Oguchi, 2005), the procedure is time consuming (involving the removal of the

* Corresponding author.
E-mail addresses: tristan.roussillon@univ-lyon2.fr (T. Roussillon), herve.piegay@ens-lsh.fr (H. Piégay).

0098-3004/$ - see front matter © 2009 Elsevier Ltd. All rights reserved.
doi:10.1016/j.cageo.2009.01.013

particle, washing, and a 20+ min scan), an automatic computation of Wadells index in the maximum projection plane is a good trade-off between accuracy and time spent in the field. Although several methods have been proposed that provide an estimate that is linearly correlated with the values given by Krumbein's chart, a method that automatically calculates Wadell's original index has not yet been developed.

One of the roundness determination methods is based on the Fourier transform. A well-known method has been proposed by Diepenbroek et al. (1992). This method takes as input the polar coordinates of a sample of 64 points of the particle boundary, spaced at equal angular intervals. The Fourier transform is computed from the distance to the centroid. The weighted sum of the amplitudes of the first 24 coefficients of the Fourier transform is a roundness estimate. To remove size information, the coefficients are divided by the zeroth coefficient. In addition, sphericity aspect is eliminated by subtracting the spectrum of the best approximating ellipse from that spectrum. The measure obtained was found to be linearly correlated (94%) with the values of Krumbein's chart. They then applied their method to address fluvial and nearshore transport processes in Calabria, with the measurement of around 20,000 gravels of different lithology.

An alternative method using mathematical morphology was proposed by Drevin and Vincent (2002). The idea is to apply a morphological opening on a particle silhouette. The morphological opening consists of an erosion and a dilation with a same structuring element, so that some shape features like 'cape' or 'isthmus' are removed without a contraction of the silhouette. The ratio between the particle area before and after the morphological opening is a roundness measure again linearly correlated (96%) with the values of Krumbein's chart, with a circular structuring element of radius equal to 42% of the radius of the largest inscribed circle.

The aim of this paper is to develop a method to automatically calculate Wadell's pioneering roundness index on the maximum projection plane (Wadell, 1932), as well as the index of Drevin and Vincent (2002). We will also develop new indices based on particle geometry to study roundness with respect to form and size, notably the ratio between perimeters of the silhouette and of the best approximating ellipse, which has been positively correlated to the values of Krumbein's chart. As we choose to focus on geometrical parameters, we do not implement parameters that use signal processing like the index proposed by Diepenbroek et al. (1992). This work should help to accelerate the sediment sampling process in river studies and allow the development of geographical hypotheses related to sediment particle roundness at the river network scale.

This paper is organised as follows. In Section 2, we describe the shape parameters we implemented and give some details about the implementation of Wadell's index. In Section 3, we compare different shape parameters using Krumbein's chart. Experiments are described in Section 4 with real images. Conclusions and future research directions are presented in Section 5.

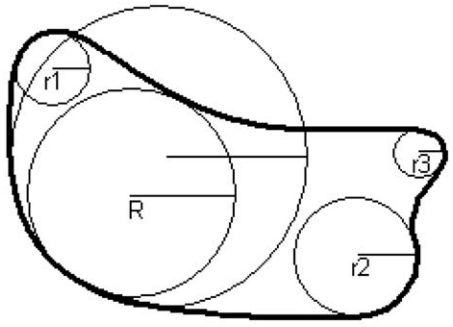

Fig. 1. Roundness definition (Wadell, 1932). On one hand, radii $r1$–$r3$, being smaller than radius R of the largest inscribed circle, define and measure corners. On other hand, circle without label, being greater than radius R of the largest inscribed circle, does not define nor measure a corner. As a consequence, roundness is the average of $r1$–$r3$.

2. Computation of shape parameters using discrete geometry

In this section we consider a binary image of a pebble. The image has been taken such that it coincides with the maximum projection plane of the pebble (this is what we called the *silhouette* of the particle in Fig. 3). From this silhouette we compute one size parameter and some form and roundness parameters.

2.1. Size parameter

Traditionally, the most frequently used size parameters are the lengths of the three representative axes: a (major axis), b (medium axis), c (minor axis). Using the rotating calipers algorithm (Toussaint, 1983), a basic tool of computational geometry

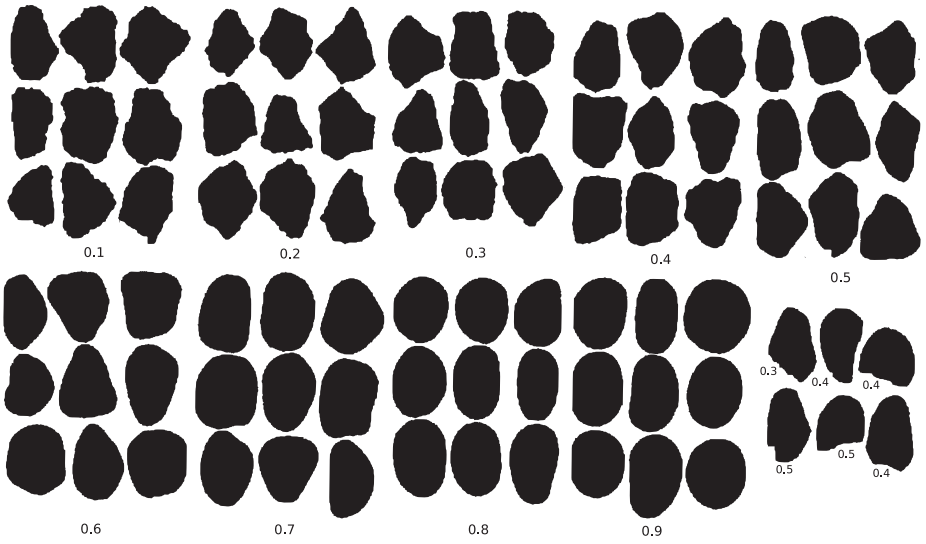

Fig. 2. Krumbein's chart (Krumbein, 1941).

Please cite this article as: Roussillon, T., et al., Automatic computation of pebble roundness using digital imagery and discrete geometry. Computers and Geosciences (2009), doi:10.1016/j.cageo.2009.01.013

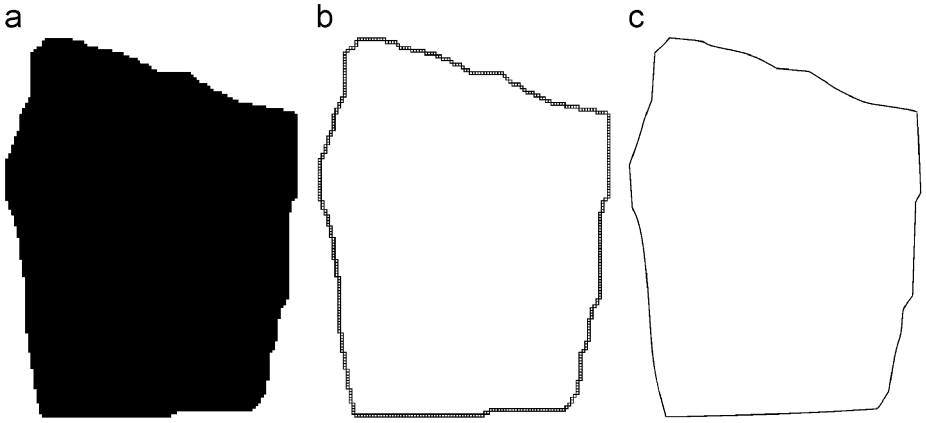

Fig. 3. Silhouette of a particle shown in (a) and its boundary in (b). Polygonalisation of boundary is in (c).

(Preparata and Shamos, 1985), we can easily estimate a and b from the silhouette of a particle. The idea is to rotate two parallel lines around the silhouette, such that the silhouette is enclosed by the two lines and the two lines touch the silhouette: a is the maximum distance between such parallel lines and b is the minimum distance between such parallel lines. We take b as a measure of the particle size, the so-called b-axis of the particles (Bunte and Abt, 2001).

2.2. Form parameters

Circularity, defined as the ratio between the perimeters of the silhouette and of a disk of same area as the silhouette, is a basic descriptor in digital image analysis. It can be seen as a two-dimensional equivalent of sphericity. If P_S and A_S denote, respectively, the perimeter and the area of the silhouette, the formula is

$$circularity = \frac{P_S}{2\sqrt{A_S \pi}} \tag{1}$$

Before computing the perimeter and area of the silhouette, we extracted the boundary of the silhouette by contour tracking and we polygonalised the sequence of 8-connected pixels with a digital straight segment recognition algorithm (Debled-Rennesson and Réveillès, 1995) (Fig. 3). Next, the area and perimeter were computed from the obtained polygon.

From a theoretical point of view, we used the arithmetical definition of the digital straight line, which leads to an algorithm that is linear in time with integer-only computations. In addition, it is proven that if the image resolution is infinitely high, then the perimeter and area estimations are infinitely close to the true values (Klette and Zunic, 2000).

However, *circularity* is difficult to interpret because it confounds size, elongation, convexity and roundness information. We propose to study these parameters independently and their definitions are given hereafter:

Elongation is easy to compute and is equal to the ratio between b and a

$$elongation = \frac{b}{a} \tag{2}$$

Convexity is defined as the ratio between the area of the silhouette (A_S) and of the convex hull of the silhouette (A_{CH}). A convex hull is defined as the minimal convex polygon covering of an object. The convex hull has been thoroughly studied in computational geometry (Preparata and Shamos, 1985) and is computed here with the algorithm of Melkman (1987)

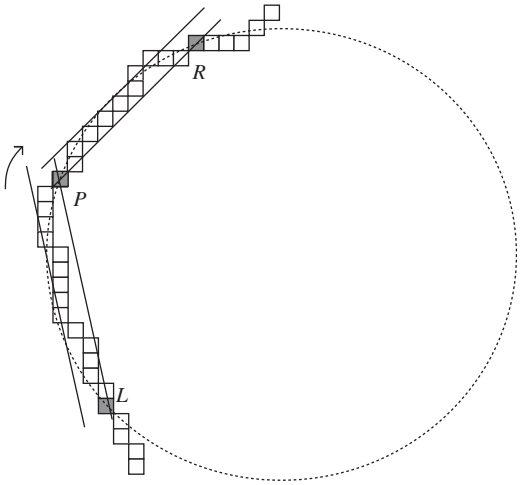

Fig. 4. Example of computation of radius of curvature at a pixel P. Radius of curvature is radius of the circle (dotted line) passing through LPR.

$$convexity = \frac{A_S}{A_{CH}} \tag{3}$$

2.3. Roundness parameters

Wadell defined his roundness index as follows:

$$rW = \frac{1}{k.R}\sum_{i=1}^{k} r_i \tag{4}$$

where r_i is the radius of curvature that is smaller than or equal to the radius of curvature R of the largest inscribed disk at a pixel on the boundary of the pebble silhouette and k is the number of such radii.

The implementation of rW followed three steps:

(1) The radius of curvature at each pixel was estimated in a robust way using an algorithm illustrated in Fig. 4 (Nguyen and Debled-Rennesson, 2007).
First, the longest sequences of 8-connected pixels lying between two parallel straight lines separated by a given distance d to the left and to the right of P were identified. In Fig. 4 and hereafter $d = 2$. The end of the sequence of 8-connected pixels to the left (resp. to the right) of P is

Please cite this article as: Roussillon, T., et al., Automatic computation of pebble roundness using digital imagery and discrete geometry. Computers and Geosciences (2009), doi:10.1016/j.cageo.2009.01.013

denoted by L (resp. R). Next, the radius of the circumcircle of the triangle LPR was computed. This procedure was repeated for each pixel.
Note that the above method is more accurate than the original one because a continuum of radii is considered instead of a class of concentric circles of fix radius (Barrett, 1980).

(2) The radius of the largest inscribed disk is calculated using the distance transform of the silhouette. The distance transform is a frequently used tool in discrete geometry that consists of labelling each pixel of the silhouette by its distance to the nearest pixel not belonging to the silhouette (Fig. 5). It was computed using the efficient algorithm of Hirata (1996).

(3) rW was calculated using Eq. (4). Only the pixels with a radius of curvature smaller or equal than the radius of curvature of the largest inscribed disk were taken into account (Fig. 6).

For comparison, we also calculated the roundness measure proposed by Drevin and Vincent (2002). This parameter is also geometrical because the basic morphological operations are related to the distance transform, the tool used to compute the radius of the largest inscribed disk

$$rD = \frac{A_{S \oplus C(o,r_c) \ominus C(o,r_c)}}{A_S} \quad (5)$$

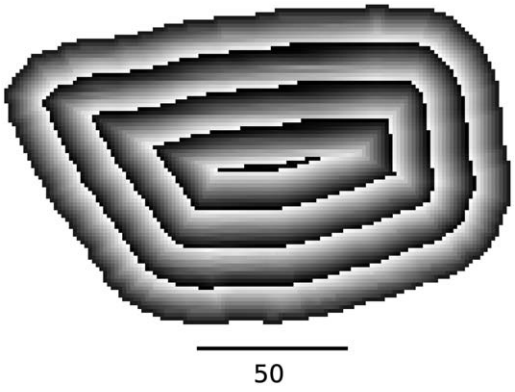

Fig. 5. Distance transform of a pebble silhouette. Each pixel is filled with a gray level according to its distance to nearest pixel not belonging to silhouette (modulo 10). Radius of largest inscribed circle is 40.6.

where $A_{S \oplus C(o,r_c) \ominus C(o,r_c)}$ denotes the area of the silhouette after a morphological opening with a circular structuring element C of center o and radius r_c. As in Eqs. (1) and (3), A_S denotes the area of the silhouette. Operators $\oplus$ and $\ominus$ denote Minkowski's addition (dilatation or thresholding in the distance transform of the complementary set of the silhouette) and Minkowski's subtraction (erosion or thresholding in the distance transform of the silhouette), respectively. The radius r_c of the circular structuring element was fixed to 75% of the radius R of the largest inscribed disk. This is the percentage for which rD had the best correlation with the values of Krumbein's chart (Section 3).

As stated above, we chose to focus on geometrical parameters and therefore we do not implement parameters based on signal processing like the one proposed by Diepenbroek et al. (1992).

Finally, because it has been previously correlated to Wadell's index (Cottet, 2006), we also computed the ratio between the perimeter of the sihouette (P_S) and of the best approximating ellipse (P_e) as a last roundness measure as follows:

$$rP = \frac{P_S}{P_e} \quad (6)$$

Since *circularity*, which consists in comparing the silhouette with a circle, includes both size, elongation and roundness information, the idea is to compare the silhouette with an ellipse, instead of a circle, to remove size and elongation aspects and capture only the roundness.

2.4. Behavior of shape parameters with respect to resolution

In this section, the behavior of our shape parameters is studied with respect to resolution. We used synthetic images, so that the resolution was controlled and the true values of our shape parameters were known.

We assumed an orthogonal grid with a uniform spacing denoted by l between the grid points. We assumed that in a digital image, pixels are grid points. The resolution of the image r is defined as $r = 1/l$. Geometrical shapes were digitised such that pixels located inside and outside the shape were labelled *object* and *background*, respectively. To increase the resolution r, we may shrink the grid as well as leave the grid fixed and dilate the shape (Klette and Zunic, 2000). Therefore, the shape parameters introduced above were computed on digitised ellipses of increasing size (Fig. 7). An ellipse was used instead of a polygon (or a

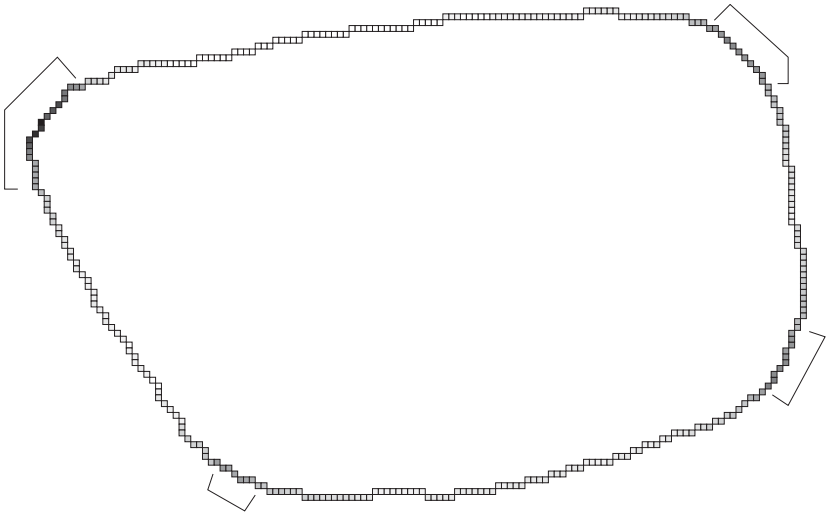

Fig. 6. Radius of curvature, which is computed for each pixel. The darker the pixel, the smaller the radius of curvature. Only pixels whose radius of curvature is less than the radius of largest inscribed circle are taken into account in roundness calculation. Roundness is the ratio between average of radius of curvature of retained pixels (28.5) and radius of largest inscribed circle (40.6), that is, 0.70.

Please cite this article as: Roussillon, T., et al., Automatic computation of pebble roundness using digital imagery and discrete geometry. Computers and Geosciences (2009), doi:10.1016/j.cageo.2009.01.013

circle that is a specific case of the ellipse), because most of parameters, which are based on digital straight segment recognition (*circularity*, *convexity*, *rP*, *rW*), are more accurate when the geometrical shape is a polygon and an ellipse thus allowed us to test the worst-case scenario.

The curves of three of the five parameters (*convexity*, *circularity*, *rP*) are quite smooth and converge very quickly toward the true values (1, approximately 0.83 and 1, respectively). These parameters are computed thanks to very accurate perimeter and area estimators. The curves of the two others (*rD* and *rW*) are less smooth and converge more slowly to constant values as the size of the digitised ellipses increases. The true values of *rD* and *rW* are difficult to compute. However, a coarse estimation of ground-truth (e.g. around 0.6 or 0.65 for *rW*) as well as the accuracy of the tools used for the computation (an exact euclidean distance transform and a robust curvature estimation for *rW*) allows confidence that the computed values approach the true values.

The above analysis suggests that to remove the influence of the resolution, a silhouette minimum size has to be used. To do so, a threshold on the shape perimeter is set: beyond this threshold, the error is considered acceptable. In Fig. 7, the error is less than 10% for all shape parameters above a perimeter of 150 pixels. We conclude that measures are accurate for all shape parameters, if the perimeter of the extracted boundary of each pebble is above this value.

3. Correlations study using Krumbein's chart

In Table 1, the correlation between the individual mean values of the shape parameters and Krumbein's chart roundness values is given in columns 2 and 3, respectively.

While the new roundness parameters should preferably be tested on real-world data rather than Krumbeins chart silhouettes following Diepenbroek et al. (1992) and Drevin and Vincent (2002), it is also useful to compare the estimates of Wadells index from our algorithm to Krumbeins chart roundness values.

Our implementation of Wadell's index is the shape parameter that provides the best results with a linear correlation of 92%. This is reassuring since Krumbein (1941) used the method proposed by Wadell (1932) to divide his standard profiles into nine classes having the same roundness value (Section 1). Table 1 also shows that the form parameters of *circularity*, *convexity* and *rP* are also linearly correlated with Krumbein roundness values. However, the correlation coefficients found are lower than the values given in the literature (Section 1). For instance, our implementation of Drevin's parameter provides a linear correlation of 85% compared to 96% in Drevin and Vincent (2002). The discrepancy may be related to the differences of implementation (our distance transform is not an approximation but is exact) and of quality of the input image (quality of Krumbein's chart, acquisition process, resolution, and so on).

In Fig. 8, *rW* is plotted against the Krumbein roundness classes (*rK*). The slope of the least square regression line is greater than 2, whereas its *y*-intercept is around of −0.7, which conflicts with the

Table 1
Correlation between shape parameters values and Krumbein's chart ones (*b*: size, *b*/*a*: elongation, *rD*: Drevin's roundness, *rW*: Wadell's roundness, *rP*: ratio between perimeters of the silhouette and of the best approximating ellipse).

Shape parameters	Correlation coefficient	
	Individual values ($n = 81$)	Mean values ($n = 9$)
b	0.065	0.153
b/*a*	0.057	0.199
rD	0.847	0.967
rW	**0.919**	**0.992**
rP	0.899	0.979
Circularity	−0.844	−0.984
Convexity	0.895	0.972

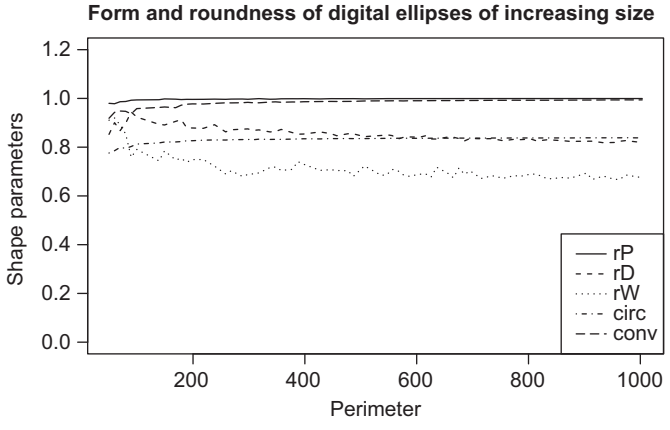

Fig. 7. Shape parameters introduced in Section 2 (*circ*: circularity, *conv*: convexity, *rD*: Drevin's roundness, *rW*: Wadell's roundness, *rP*: ratio between perimeters of sihouette and of best approximating ellipse) over perimeter of digital ellipses. A digital ellipse is the set of pixels, center of which is located inside a euclidean ellipse. Elongation of digital ellipses is fixed and equals 1/2, whereas perimeter ranges from 10 to 1000.

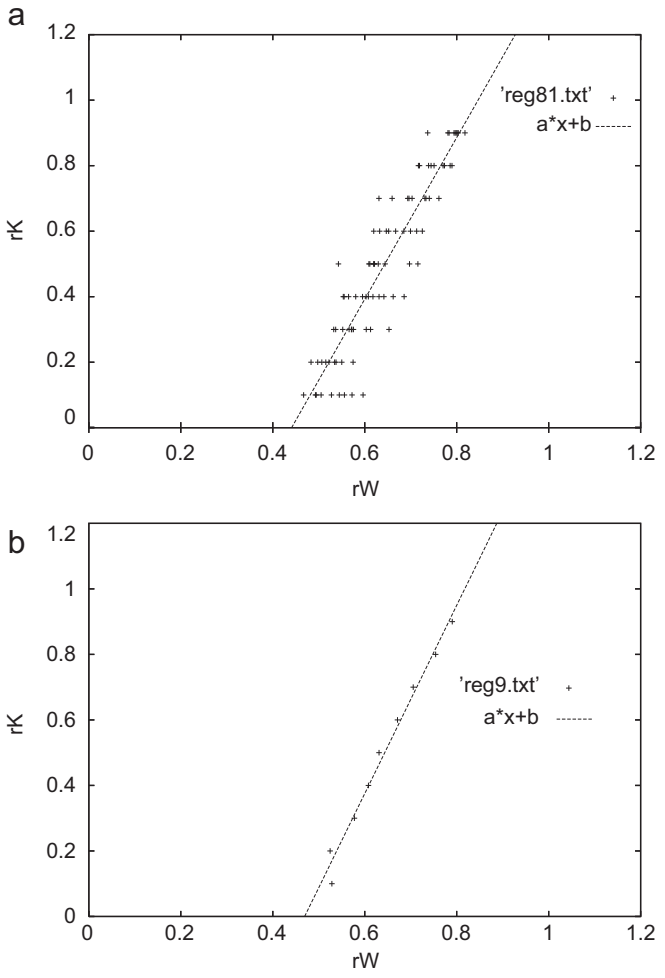

Fig. 8. Correlation between *rW* and Krumbein roundness classes (*rK*) computed on individual values in (a) (each cross depicts a silhouette of Krumbein's chart) and on mean values in (b) (nine crosses depict the nine roundness classes of Krumbein's chart).

Please cite this article as: Roussillon, T., et al., Automatic computation of pebble roundness using digital imagery and discrete geometry. Computers and Geosciences (2009), doi:10.1016/j.cageo.2009.01.013

expected slope of 1 and y-intercept of 0. Intraclass variance is higher than expected whereas interclass variance is lower than expected. The source of this variance is the lack of corner and curvature definitions in the original paper of Wadell (1932) (Section 1). This methodologic gap could also explain the high inter-observer variability of Cailleux roundness index noticed in Pissart et al. (1998).

4. Assessment of the longitudinal pattern of particle abrasion

We used our shape parameters in order to study real pebbles from digital images, collected in the bed of the Progo, an Indonesian river located on Java Island near Yogyakarta. The river is 135 km long, has a catchment of 2400 km^2 and drains several volcanos, such as the Merapi, still active on the east side (2900 m in elevation) and also the Sumbing and the Sundoro on the west side (3200 and 3100 m in elevation, respectively). The source of the river is on the northern side of Mount Sundoro at 2500 m in elevation (Fig. 9). Two thousand five hundred pebbles of andesic were randomly sampled in the bed, with 2–5 photos being taken on 25 stations located at various distances from the source (in average every 5 km). We analysed an average of 105 pebbles per station (min = 73; max = 154). Digitised pebble boundaries varied between 150 and 620 pixels (mean: 330 ± 70 pixels).

In a first step we detected pebbles with clustering methods, transforming the original color image into a binary image as shown in Fig. 10. In a second step, we extracted the boundaries from pebbles silhouettes to compute the shape parameters described in Section 2. For each sample of pebbles (around 100 pebbles per sample), characterised by its distance from the source, we computed the average value of each shape parameter and their confidence level at $\alpha = 0.05$.

To compare the stations along the river, we selected similar size classes, from very coarse gravels to small pebbles (Bunte and Abt, 2001). The 10th and 90th percentiles of the samples are,

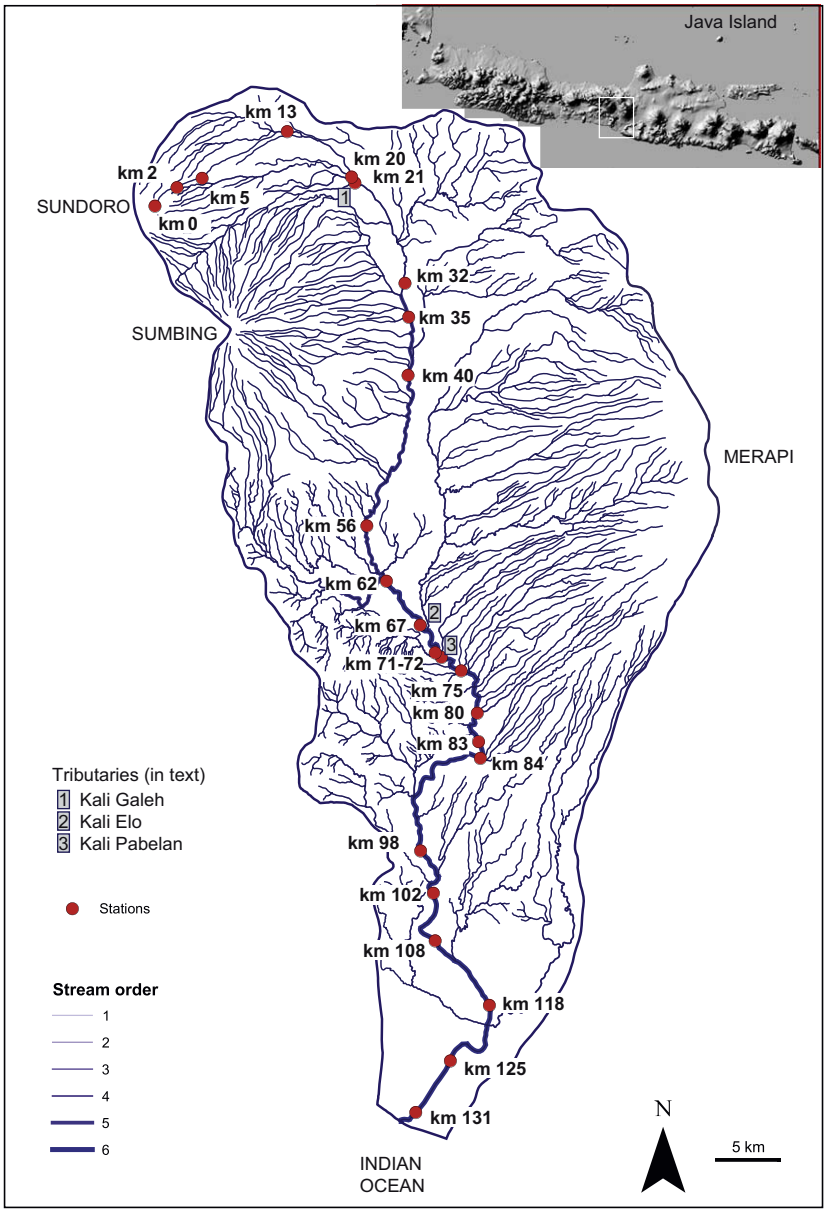

Fig. 9. Catchment of Progo River, Java Island, Indonesia. Note the structure of hydrographic network that is strongly controlled by volcanoes. Twenty-five stations are located along the main stem from Sundoro volcano to Indian Ocean and their distances to the source (in km) are indicated.

Please cite this article as: Roussillon, T., et al., Automatic computation of pebble roundness using digital imagery and discrete geometry. Computers and Geosciences (2009), doi:10.1016/j.cageo.2009.01.013

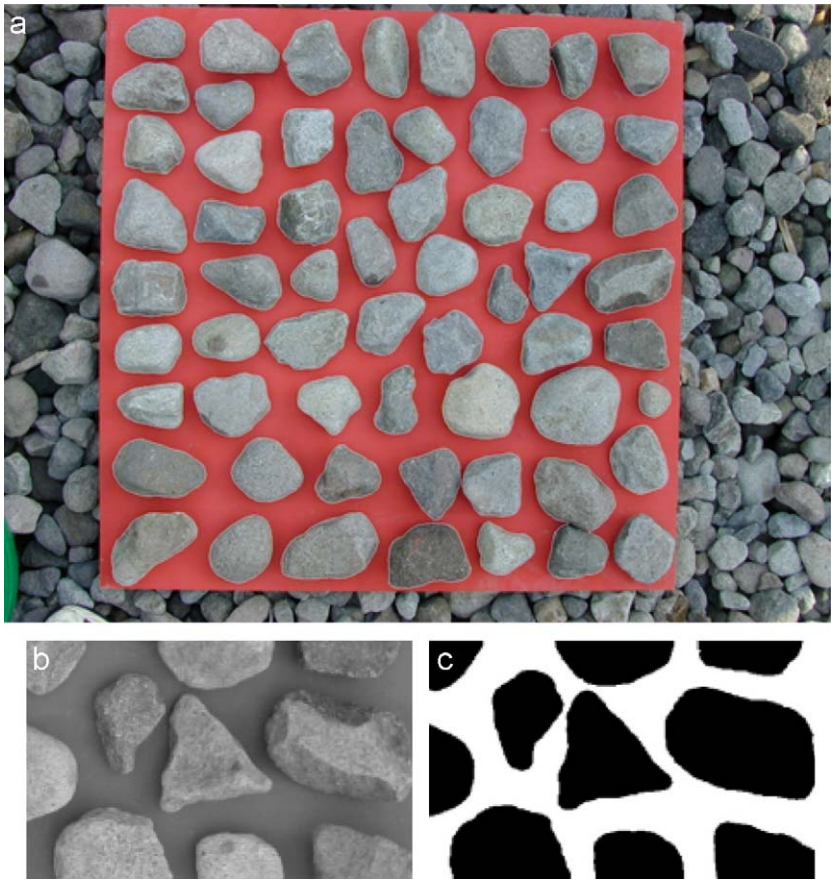

Fig. 10. An image of sample pebbles with boundaries extracted in white (a). Extraction is performed by contour tracking in binary image (b). Last is computed with clustering methods applied to the original color image (c).

respectively, 51 and 87 mm in *b*-axis. ANOVA tests to evaluate the independence of average *b*-axis values showed that stations are not statistically different at $\alpha = 0.05$, except stations located 56 and 84 km which are significantly coarser particles than the others.

Fig. 11 depicts the longitudinal pattern of each parameter along the river course. The different parameters do not show a well-structured trend from the mouth to the ocean, which demonstrates the complex origin of the particles located in the main stem. The clearest longitudinal trend was obtained by the convexity ($r^2 = 0.035$). While each parameter has a unique pattern, *rP* and *circularity* are highly correlated (the coefficient of determination r^2 equals -0.928) as are *convexity* and *circularity* ($r^2 = -0.899$). *rW* is the parameter that is the most least correlated with the others. The best correlation is observed for *rD*($r^2 = 0.76$) and the coefficient of determination is less than 0.63 for the three others. A similar general pattern can be nevertheless observed from most of the parameters:

(1) Angular particles are preferentially observed in the upstream section with a clear trend in roundness development from 0 to 20 km for *rP*, *rD*, *convexity* and *circularity*, and until 50 km for *rW*. Therefore, the least round particles are generally observed at the source station (*rW*, *rD*, *circularity*, *convexity* and *rP* parameters).
(2) For all parameters, a significant decrease in roundness is also observed in the middle of the section (60–80 km).
(3) Downstream of 80 km, all of the parameters exhibit a significant increase in roundness until 100 km but then, they are fairly constant until 130 km. With the exception of *rW*, the roundness estimates are here similar or slightly higher (*convexity* and *rP*) than those observed between 25 and 50 km. The most rounded particles are observed at the downstream station or close to it (*rP*, *circularity*, *convexity*). Downstream, *rW* does not readjust to the disruption that occurs in the middle section and does not reach the highest values until around 50–55 km.

From a thematic point of view, a nice trend in roundness is observed in the upstream part of the catchment. This trend is clear because no main tributary providing less rounded particles disrupts the abrasion process. The delivery of the Kali Galeh at 21 km is the only perturbance detected by some of the parameters but it does not counteract the trend. It is then possible to fit a law for predicting roundness process in such an andesitic environment using *rW* ($rW = 0.002\,\text{km} + 0.69; r^2 = 0.87$) or *rP* parameter ($\log(\text{rP}) = 0.009\,\log(\text{km}) + 0.69; r^2 = 0.90$). These results also underline that such parameters are powerful enough to determine a roundness trend over long distances (e.g. 20–50 km) whereas previous work had indicated that roundness only significantly affected particles near the source (the first km) after which it was constant in a downstream direction (Pissart et al., 1998, for example). The parameters are also robust enough to highlight the major disruption in the roundness trends due to sediment delivery in the middle section from the active Merapi volcano located on the east side. This area is a major source of angular material that disrupt the longitudinal trend. The distance from the peak of Merapi to the main stem is only 25–30 km. It is then

Please cite this article as: Roussillon, T., et al., Automatic computation of pebble roundness using digital imagery and discrete geometry. Computers and Geosciences (2009), doi:10.1016/j.cageo.2009.01.013

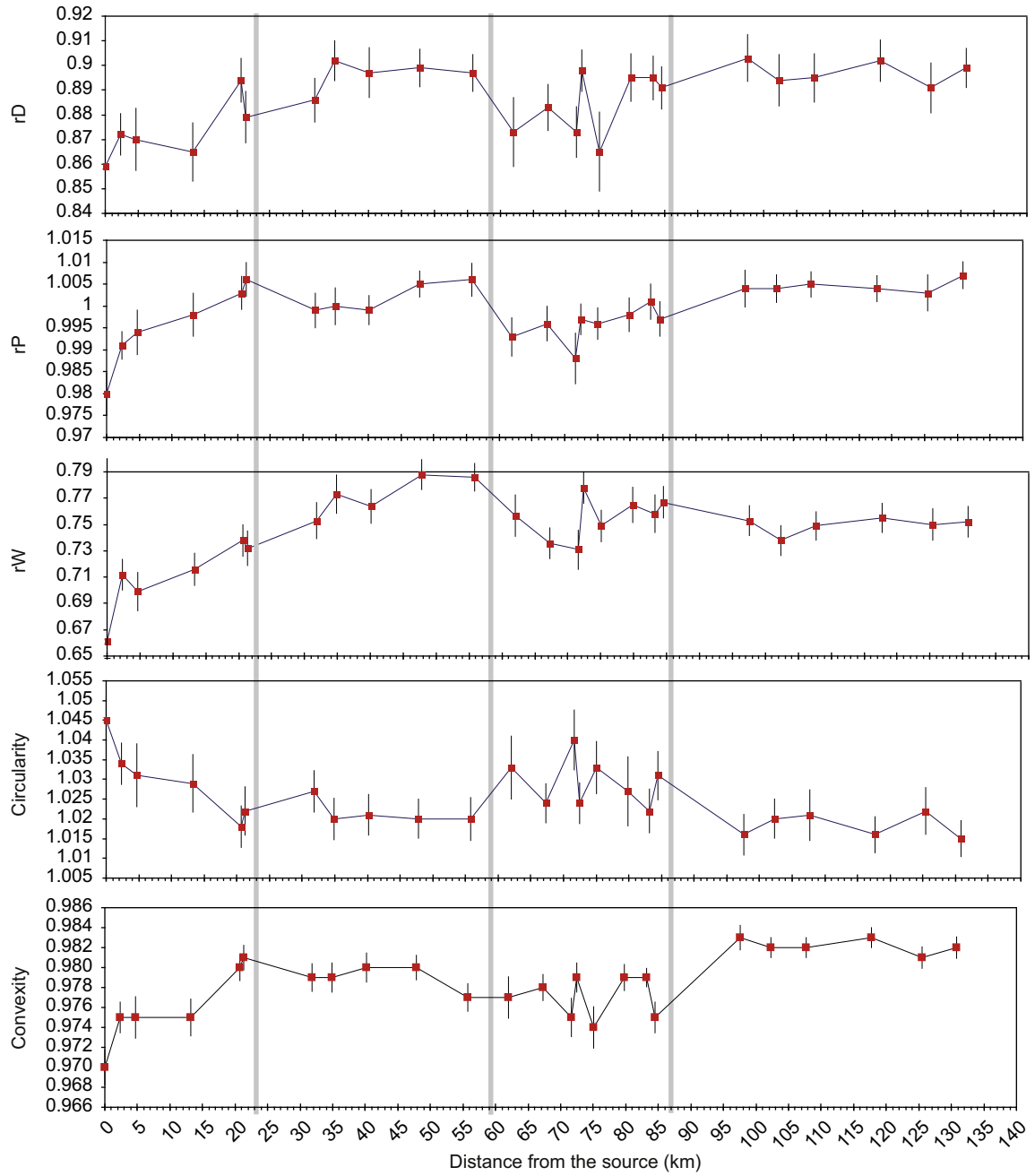

Fig. 11. Longitudinal pattern of our implementation of Wadell's method (*rW*), Drevin's method (*rD*), perimeter ratio (*rP*), *circularity* and *convexity* from the source of Progo (0 km) to the ocean (130 km).

interesting to see that the *rW* and *rD* values reached in this section (60–80 km) are then very similar to those observed at 25–30 km of the main stem, which may indicate that the abrasion process on the Merapi slopes is similar to that observed on the Sandoro, which is a much older volcano. The decrease in roundness already occurs by the 62 and 67 km stations, which is before the confluence with the Kali Elo and Kali Pabelan that drain the Merapi. This indicates that the delivery is not only linked to the river network itself but also from inherited material provided by the Merapi, stored in the alluvial corridor and delivered by bank erosion. The trends observed downstream the area influenced by the Merapi are more difficult to interpret because the different indicators have contrasting patterns. This raises the possibility of using the different parameters in combination in order to characterise the abrasion process over a long continuum and the possible substitution of macro-scale for micro-scale shape changes as the particle abrades over distances longer than a few kilometers. In the downstream context of the Progo basin, some parameters, mainly *circularity* and *convexity*, may be more powerful for characterising roundness trend when particle corners are already smoothed. We may then hypothesise that *rW* would be a better discriminant parameter of roundness upstream in a context of angular particles whereas *rP*, *convexity* and *circularity* would be more powerful downstream when the particle corners are already smoothed and the abrasion affects the shape itself.

5. Conclusion and perspectives

These new computer developments are a powerful tool to better understand in field abrasion processes. The automatic imagery

Please cite this article as: Roussillon, T., et al., Automatic computation of pebble roundness using digital imagery and discrete geometry. Computers and Geosciences (2009), doi:10.1016/j.cageo.2009.01.013

procedure allows us to replace the easy-to-collect indices such as Krumbein visual classes and the Cailleux index with the more precise roundness parameter, *rW*. From this preliminary field analysis, it is clear that the implementation of the *rW* parameter is useful because, unlike other parameters that are more sensitive to the particle shape, it quantifies the corner shapes of particles. By providing both corner and shape parameters, the developments allow us to study the abrasion process over a long spatial continuum. We can expect that *rW* is the most robust parameter closer to the source as it is based on all the corners and describes the corner abrasion, whereas *rP*, *convexity* or *circularity* provide indications at a macro-scale of abrasion effects on the particle shape. The field example has been based on average values, but a multivariate analysis is a challenging issue that could better explore the variability of roundness parameters observed at each of the stations and its evolution downstream.

It has also been shown that the resolution may affect the quality of the results but that the parameters are fairly robust and allow the comparison of pebbles of various sizes from the photos of different resolutions. Threshold values in terms of resolution (e.g., number of pixels per pebble perimeter) are provided to correctly specify the field collection requirements in terms of photo resolution and minimum particle size.

In the future, other indices such as the roundness of the sharpest corner, which reflects the most recent transport conditions (Barrett, 1980), could be studied instead of the average roundness of particle corners. Moreover, as Wadells index has been implemented with a continuum of radii of curvatures, the available amount of quantitative information is greater than that provided by the visual analysis of Krumbeins chart. Different measurements such as the roundness of the sharpest corners, the average and the standard deviation of the roundness of the corners could be used to better evaluate differences in geographical responses.

In order to check the hypothesis according to which the most outstanding corners of particles are more likely to be abraded than others, it would be interesting to investigate the longitudinal pattern of the roundness measure of individual corners (instead of whole particles) along the river course. This could help to introduce other indices where the corners are weighted depending on their position on the particle outline. This kind of index should be more clearly representative of abrasion processes during transport than our implementation of Wadell's index.

For testing the computer programs, we worked with a homogeneous lithology. The identification and analysis of multiple lithologies is also a challenging issue for which it may be possible to implement computer programs. In order to develop such approaches, a clear understanding of sediment budgeting and sediment source locations is needed before exploring the effect of lithology on particle changes downstream in experimental field conditions.

Acknowledgments

The authors thank Albert Pissart and an anonymous reviewer for their comments on an early version of this manuscript.

The authors also thank the different colleagues who participate to earlier discussions and debates about characterising pebble roundness and shapes from imagery processing, notably Bernard Lacaze from Prodig, Paris, and Christophe Delacourt from the University of Brest. The experimental sample has been collected in an International Program of Scientific Cooperation led by Franck Lavigne: PICS 1042 "Dynamique sédimentaire et risques naturels dans le bassin du fleuve Progo, Java Centre, Inonésie" (2001–2003). The authors also thank Bruce MacVicar for his careful proofreading.

This work has been partially supported by a grant from the DGA for Tristan Roussillon.

References

Barrett, P.J., 1980. The shape of rock particles, a critical review. Sedimentology 27, 291–303.

Bunte, K., Abt, S.R., 2001. Sampling surface and subsurface particle-size distributions in wadable gravel- and cobble-bed streams for analyses of sediment transport, hydraulics, and streambed monitoring. General Technical Report RMRS-GTR-74, Fort Collins, CO: U.S. Department of Agriculture, Forest Service, Rocky Mountain Research Station, p. 428.

Cailleux, A., 1947. L'indice d'émoussé: définition et première application (Roundness index: definition and first application). Compte-rendu sommaire de la Société géologique de France 13, 251–252.

Cottet, M.L., 2006. Mesure et structures spatiales et temporelles de l'émoussé des galets dans le réseau hydrographique du Bez (On the measurement, the spatial and temporal distribution of pebble roundness in the hydrographic network of the Bez). Unpublished M.Sc. Thesis, Université Jean Moulin Lyon 3, Lyon, France, p. 72.

Debled-Rennesson, I., Réveillès, J.-P., 1995. Linear algorithm for segmentation of digital curves. International Journal of Pattern Recognition and Artificial Intelligence 9, 635–662.

Diepenbroek, M., Bartholomä, A., Ibbeken, H., 1992. How round is round? A new approach to the topic 'roundness' by Fourier grain shape analysis. Sedimentology 39, 411–422.

Drevin, G.R., Vincent, L., 2002. Granulometric determination of sedimentary rock particle roundness. In: Proceedings of International Symposium on Mathematical Morphology, Sydney, Australia, pp. 315–325.

Hayakawa, Y., Oguchi, T., 2005. Evaluation of gravel sphericity and roundness based on surface-area measurement with a laser scanner. Computers & Geosciences 31, 735–745.

Hirata, T., 1996. A unified linear-time algorithm for computing distance maps. Information Processing Letters 58 (3), 129–133.

Klette, R., Zunic, J., 2000. Multigrid convergence of calculated features in image analysis. Journal of Mathematical Imaging and Vision 13, 173–191.

Krumbein, W.C., 1941. Measurement and geological significance of shape and roundness of sedimentary particles. Journal of Sedimentary Petrology 11 (2), 64–72.

Melkman, A.A., 1987. On-line construction of the convex hull of simple polygon. Information Processing Letters 25 (11), 11–12.

Nguyen, T.P., Debled-Rennesson, I., 2007. Curvature estimation in noisy curves. In: Proceedings of the 12th International Conference on Computer Analysis of Images and Patterns, Vienna, Austria, pp. 474–481.

Pissart, A., Duchesne, F., Vanbrabant, C., 1998. La détermination pratique des intervalles de confiance des comptages de cailloux et des mesures d'émoussé. Comparaison des mesures d'émoussé de Cailleux et de Krumbein (The practical determination of confidence intervals for counting pebbles and roundness measures. Comparison of the roundness indices of Cailleux and Krumbein). Géomorphologie: Relief, Processus, Environnement 3, pp. 195–214.

Preparata, F.P., Shamos, M.I., 1985. Computational Geometry: An Introduction. Springer, New York, p. 390.

Toussaint, G.T., 1983. Solving geometric problems with the rotating calipers. In: Proceedings of the 2nd IEEE Mediterranean Electrotechnical Conference, Athens, Greece, pp. A10.02/1–4.

Wadell, H., 1932. Volume, shape, and roundness of rock particles. Journal of Geology 40, 443–451.

Please cite this article as: Roussillon, T., et al., Automatic computation of pebble roundness using digital imagery and discrete geometry. Computers and Geosciences (2009), doi:10.1016/j.cageo.2009.01.013